

## Can large wind farms affect local meteorology?

S. Baidya Roy and S. W. Pacala

Department of Ecology and Evolutionary Biology, Princeton University, Princeton, New Jersey, USA

R. L. Walko

Department of Civil Engineering, Duke University, Durham, North Carolina, USA

Received 11 March 2004; revised 9 July 2004; accepted 20 July 2004; published 1 October 2004.

[1] The RAMS model was used to explore the possible impacts of a large wind farm in the Great Plains region on the local meteorology over synoptic timescales under typical summertime conditions. A wind turbine was approximated as a sink of energy and source of turbulence. The wind farm was created by assuming an array of such turbines. Results show that the wind farm significantly slows down the wind at the turbine hub-height level. Additionally, turbulence generated by rotors create eddies that can enhance vertical mixing of momentum, heat, and scalars, usually leading to a warming and drying of the surface air and reduced surface sensible heat flux. This effect is most intense in the early morning hours when the boundary layer is stably stratified and the hub-height level wind speed is the strongest due to the nocturnal low-level jet. The impact on evapotranspiration is small.

*INDEX TERMS:* 3307 Meteorology and Atmospheric Dynamics: Boundary layer processes; 3329 Meteorology and Atmospheric Dynamics: Mesoscale meteorology; 3379 Meteorology and Atmospheric Dynamics: Turbulence; 1630 Global Change: Impact phenomena; *KEYWORDS:* wind power, wind farm, renewable energy, environmental impact, climate, weather

**Citation:** Baidya Roy, S., S. W. Pacala, and R. L. Walko (2004), Can large wind farms affect local meteorology?, *J. Geophys. Res.*, 109, D19101, doi:10.1029/2004JD004763.

### 1. Introduction

[2] The growing energy demand of the expanding global economy is being adequately met by fossil fuels. However, the long-term future of these sources is in doubt because they are not renewable. Additionally, concerns have also been raised regarding the greenhouse gases and aerosols emitted by fossil fuel-based power plants [*Intergovernmental Panel on Climate Change (IPCC)*, 2001]. These issues are being addressed by developing cleaner and more efficient technologies for generating electricity. Parallel efforts are also on to switch to renewable and less polluting sources, amongst which wind power is one of the more popular choices. The potential for wind power generation, in terms of the spatial extent of high-wind regimes on Earth, is quite large [*Grubb and Meyer*, 1993; *Office of Energy Efficiency and Renewable Energy (EERE)*, 2002]. While windmills have been used by humans since antiquity, isolated windmills are probably not sufficient to economically harness this enormous potential. Large-scale wind farms, connected to existing electricity grids for efficient distribution, are required for this purpose. Small operational wind farms already exist in many different countries. Several environmental concerns associated with such wind farms, viz., noise and visual pollution and interference in avian flight paths, have been identified and actively addressed [*National Wind Coordinating Committee*, 1997; *American Wind Energy Association*, 2002].

[3] However, not much effort has been made to assess the impact of wind farms on the local meteorology. The rate at which wind farms extract energy from the atmosphere ( $\sim 1 \text{ W m}^{-2}$ ), while small compared to the kinetic and potential energy stored in the atmosphere, is comparable to time-tendency terms, e.g., rate of conversion of energy from one form to another, frictional dissipation rate, etc., in the atmospheric energy balance equation [*Peixoto and Oort*, 1992]. This indicates that it is possible for wind farms to influence atmospheric and surface processes.

[4] In this paper we use an atmospheric numerical model to study the impacts of a large virtual wind farm in the Great Plains region on the local meteorology over synoptic timescales under typical summertime conditions. Prognostic [*Ivanova and Nadyozhina*, 2000] and diagnostic [*Magnusson*, 1999; *Leclerc et al.*, 1999] models have been used to study the effect of wind turbines and wind farms on aspects of atmospheric dynamics. They show that wind turbines and farms significantly affect hub-height level wind speed and turbulence. This is the first paper to use a coupled land-atmosphere mesoscale model to explore if such wind farms can also influence atmospheric thermodynamics and surface fluxes of heat and moisture.

### 2. Numerical Experiment

#### 2.1. Atmospheric Model

[5] We use the Regional Atmospheric Modeling System (RAMS) [*Pielke et al.*, 1992; *Cotton et al.*, 2003] to simulate the effects of a hypothetical wind farm in Oklahoma. This

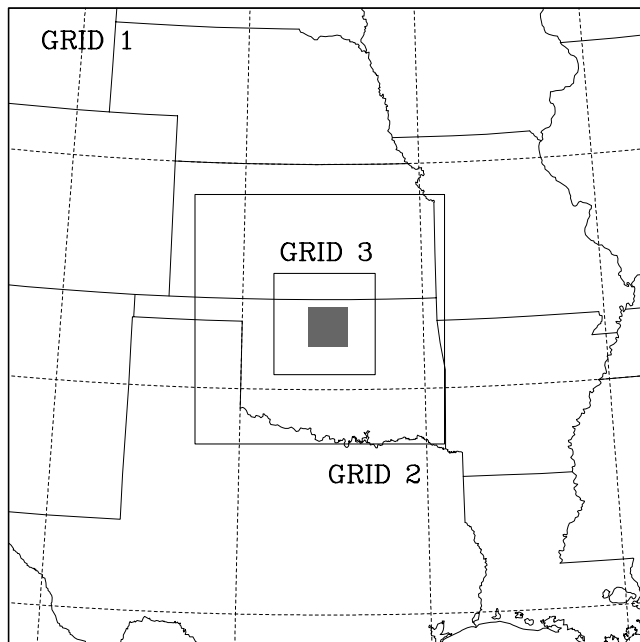


**Figure 1.** Model domain showing the three grids. The shaded area in the center of grid 3 denotes the wind farm.

region is rich in wind resources [Archer and Jacobson, 2003] and current plans recommend full exploitation of this potential [EERE, 2002].

[6] RAMS solves the full three-dimensional, compressible, nonhydrostatic dynamic equations, a thermodynamic equation and a set of microphysics equations. We close the system with the Mellor-Yamada level 2.5 scheme [Mellor and Yamada, 1982] that explicitly solves for turbulent kinetic energy (TKE) while other second-order moments are parameterized. The domain consists of 3 nested grids (Figure 1): grid 1: 1568 km  $\times$  1568 km, 32 km spacing; grid 2: 616 km  $\times$  616 km, 8 km spacing; and grid 3: 250 km  $\times$  250 km; 2 km spacing. The vertical grid is nonuniform, with higher resolution near the surface (15 levels in the lowest 2 km) to better resolve the planetary boundary layer (PBL) processes. The National Centers for Environmental Prediction/National Center for Atmospheric Research (NCEP/NCAR) reanalysis data [Kalnay et al., 1996] are used as initial and dynamic lateral boundary conditions. The land-surface boundary conditions are provided by the Land Ecosystem-Atmosphere Feedback 2 (LEAF-2) model [Walko et al., 2000].

[7] The model is run for 15 days: 1 July, 1200 UTC (0600 local time (LT)) through 16 July 1995. This is a meteorologically interesting period involving strong precipitation events early (1–3 and 5 July) followed by a dry spell. This enables us to investigate the impacts of wind farms under both wet and dry synoptic conditions. Weaver and Avissar [2001], using a setup similar to ours, have demonstrated that RAMS is capable of accurately simulating the dynamic and the thermodynamic behavior of the diurnal PBL of this region during this period.

## 2.2. Virtual Wind Farm

[8] It is computationally impossible to run a climate model at resolutions high enough to resolve turbine rotors.

So, we adopt a subgrid parameterization approach where we consider the spatially aggregated impact of several rotors on the resolved variables. Within this framework, wind farms can be approximated by increasing the surface roughness length [Ivanova and Nadyozhina, 2000; Malyshev et al., 2003]. However, in the absence of extensive field measurements, it is difficult to choose the appropriate roughness length value. Field estimates of surface roughness can be obtained from existing small wind farms but these values might not be directly applicable for large wind farms. Malyshev et al. [2003] have attempted to overcome this problem by explicitly specifying a surface drag and then calculating the corresponding roughness length by assuming neutral stability conditions.

[9] Here, we use an alternative approach which is intuitive, based on available observations and involves simple, reasonable assumptions. Since a turbine extracts energy from the atmosphere and creates some turbulence in its wake, we assume a rotor to be an elevated, massless sink of resolved kinetic energy (RKE) and source of TKE. A major advantage of this approach is that it allows us to simulate the flow both above and below the rotor, which is not possible with a surface drag approach.

[10] We assume a virtual wind farm consisting of a 100  $\times$  100 array of wind turbines spaced 1 km apart. Each turbine is 100 m tall (hub height) with 50 m long rotor blades (100 m rotor diameter). These dimensions are larger than current models but within the near-term projections for the future [EERE, 2002]. For example, the Top of Iowa Wind Farm in Worth County, Iowa, consists of turbines that are 72 m tall with 52 m rotor diameter (www.midwest-renewable.com).

[11] The coefficient of performance ( $C_p$ ) of a rotor is the fraction of available kinetic energy that it can draw from the flow. The Betz limit or the maximum possible value of  $C_p$  is 16/27 [Frandsen, 1992].  $C_p$  is a function of wind speed [Cavallo et al., 1993] but the  $C_p$  of modern commercial turbines can reach a significant fraction of the Betz limit and remain constant over a wide range of wind speeds. Rotor-generated TKE is also a weak function of wind speed. Observations from a wind farm in San Geronio, California, show that the TKE in the interior is 5–7  $\text{m}^2\text{s}^{-2}$  more than that upwind of the farm over a wide range of wind speeds (Figure 2). This wind farm is relatively small: 41 rows of 23 m tall towers with 8.5 m long rotor blades, placed approximately 120 m apart. Taylor [1983] has reported similar values.

[12] Armed with these observations, we design an experiment consisting of a control simulation and two scenarios: (1) scenario 1, where a turbine is just a sink of energy and (2) scenario 2, where a turbine acts as both an energy sink and a source of turbulence.

[13] The energy involved in the additional turbulence created in scenario 2 comes from the mean flow to satisfy the energy conservation law. We assume a constant  $C_p$  of 0.4. We also assume that at wind speeds lower than 1  $\text{ms}^{-1}$ , the rotors stop operating. This behavior is typical of all commercial turbines.

[14] The aforementioned approximations are implemented in the atmospheric model according to the following procedure. The second atmospheric layer in the model, extending from 50 m to 150 m altitudes, is 100 m thick. Within that layer we assume a cylinder with diameter = 100 m (diameter

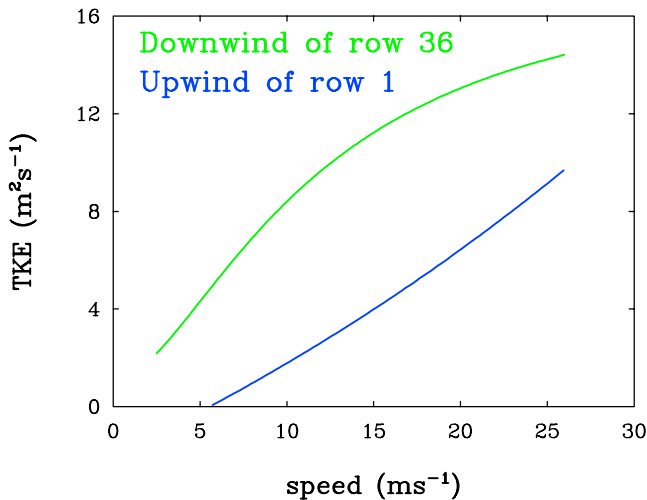


**Figure 2.** Observed 10-min averaged hub-height TKE as a function of wind speed from San Gorgonio, California.

of the turbine) and length = wind speed  $\times$  model time step. This cylinder represents the volume of air passing through a rotor in each model time step. Every time step, using the grid-resolved wind speed, we estimate the amount of RKE contained in that cylinder. If the resolved wind speed is greater than  $1 \text{ ms}^{-1}$ , we remove  $C_p$  fraction of the RKE from that cylinder in both scenarios.

[15] For scenario 2, we then calculate the amount of RKE left in that cylinder. If it is greater than  $5 \text{ m}^2\text{s}^{-2}$ , we add  $5 \text{ m}^2\text{s}^{-2}$  to the TKE in that cylinder and reduce the RKE for the cylinder by the same amount. However, if the leftover RKE is less than  $5 \text{ m}^2\text{s}^{-2}$ , we transfer all of it to the turbulent component. These operations are similar to adding a source term to the TKE equation and a sink term in the horizontal velocity equations. Since the extra TKE comes from the RKE, the energy conservation law is satisfied.

[16] The grid-resolved wind speed and TKE are then recalculated taking these operations into account. The wind farm is created by assigning 4 such cylinders per grid cell in a  $50 \times 50$  array of cells located in the center of grid 3.

[17] We note here that our assumption in scenario 2 ensures that the TKE of the volume of air passing through the rotor is up to  $5 \text{ m}^2\text{s}^{-2}$  more than the background value. In reality, turbulence decreases with distance downwind from the rotor [Petersen *et al.*, 1998]. Taylor [1983] has presented the horizontal turbulence intensity data in the wake of a single 12 m tall turbine with 17 m rotor diameter located in Aldborough, UK. On the basis of his observations, we estimate that the horizontal component of TKE 17 m downwind was  $3.7 \text{ m}^2\text{s}^{-2}$  more than the ambient, while 42.5 m downwind it was only  $1.9 \text{ m}^2\text{s}^{-2}$  higher. Thus from this perspective, it might seem that the assumption made here overestimates the effect of rotors on turbulence. However, the turbines considered in our experiment are much larger than those used to obtain the field TKE estimates and hence, generate more turbulence in their wake. This indicates that the magnitude of rotor-generated turbulence assumed in scenario 2 is probably not unrealistic.

[18] Implicit in our methodology of increasing TKE to account for rotor-generated turbulence is the assumption

that the behavior of the turbulence created by turbines is similar to that of typical boundary layer turbulence. With the limited data at our disposal, this assumption cannot be validated. However, RAMS, or other atmospheric models, do not distinguish between different sources/types of sub-grid-scale turbulence; TKE includes both convective and shear-generated turbulence. Hence, short of resolving the rotors, our methodology seems to be the only way to tackle this problem.

### 3. Results

#### 3.1. Impact of Wind Farms on Atmospheric Dynamics

[19] Wind turbines absorb energy, thereby slowing down the mean flow at the hub-height level. This is compensated by small-scale transfer of momentum from layers above and below that level. If the transport is not strong enough, the wind gradually slows down until the cutoff speed ( $1 \text{ ms}^{-1}$  in our experiment) is reached and the turbines stop. Eddies continue the restocking process and once the wind speed climbs above the threshold, they restart. In scenario 2, the wind at the hub-height level is slowed down further because a part of the energy is also consumed by turbulence. This is evident in the time series of the hub-height wind speed spatially averaged over the wind farm (Figure 3a) which shows that the speed in scenario 1 is consistently lower than that in control while scenario 2 values are even less.

[20] The difference between the cases is most stark in the early mornings (typically 0900–1000 UT (0300–0400 LT)) when the hub-height level flow is the strongest due to a nocturnal low-level jet known as the Great Plains nocturnal jet [Bonner, 1968]. This jet is defined as a thin stream of fast-moving air capping the stable nocturnal boundary layer with weak surface winds [Stull, 1988]. Under this situation, the turbines operate with high intensity as obvious from the time series of the energy extraction rate (Figure 3b). The mean power extracted over the simulation period is approximately  $0.9 \text{ Wm}^{-2}$  in scenario 1 and  $0.7 \text{ Wm}^{-2}$  in scenario 2. These values are quite close to the predicted maximum of  $1 \text{ Wm}^{-2}$  [Best, 1979].

[21] Figure 4a shows the vertical profile of wind speed spatially averaged over the wind farm and temporally averaged over the 0900 UT (0300 LT) outputs for each day. The strong positive vertical gradient due to the weak winds at the surface but the fast jet aloft is obvious. Scenario 1 shows a weakening of the flow within an approximately 500 m thick layer around the hub-height level. The wind farm in scenario 2 however, leaves a footprint that stretches beyond an altitude of 1 km. The eddies generated by the excess TKE in this case mix faster air down and slower air up which slows down the wind around the hub-height level, but also reinforces the flow near the surface, as well as aloft.

#### 3.2. Impact of Wind Farms on Atmospheric Thermodynamic Variables

[22] There is little difference in the near-surface potential temperature ( $\theta$ ) between the control and scenario 1 (Figure 3c). However,  $\theta$  in scenario 2 is generally higher than the other cases and the effect peaks during the early mornings in the dry period. Occasionally, during daytime hours, a reduction in  $\theta$  in scenario 2 can also be observed.

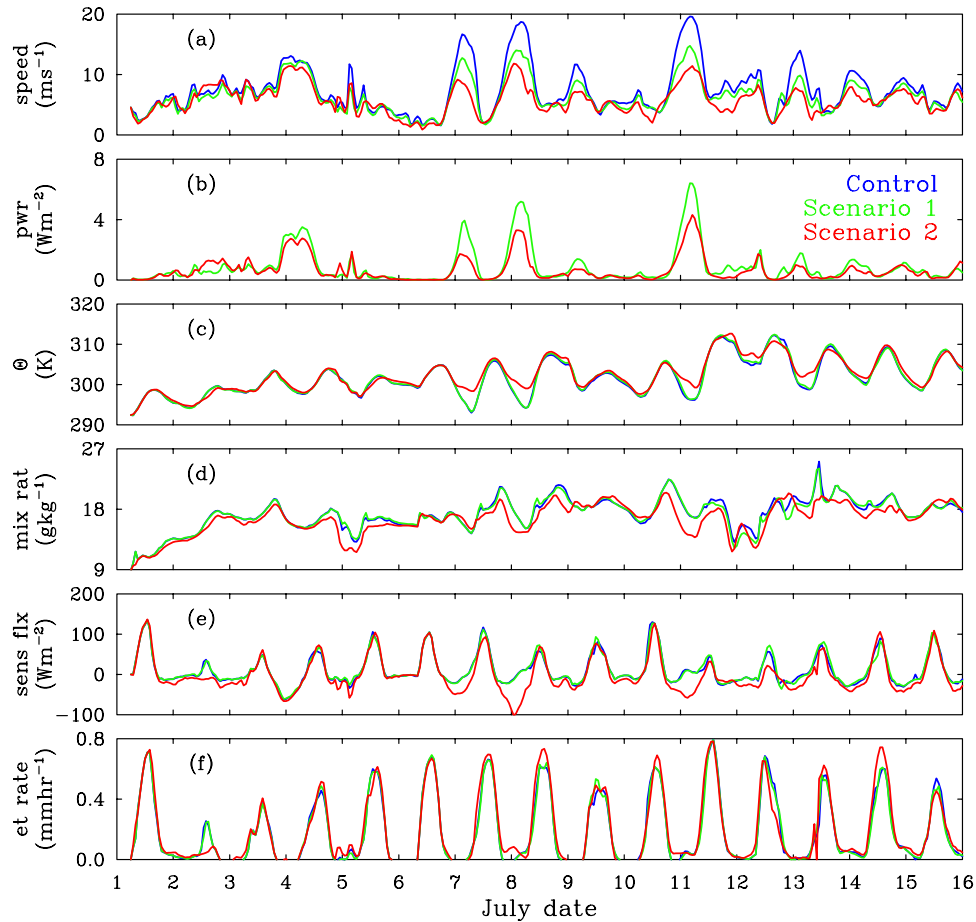


**Figure 3.** Time series of (a) hub-height horizontal wind speed, (b) power extracted, (c) surface air  $\theta$ , (d) total water mixing ratio, (e) surface sensible heat flux, and (f) surface evapotranspiration rate over the wind farm.

[23] We attempt to explain this pattern by looking at the mean  $\theta$  profile over the wind farm at 1200 UT (0600 LT) outputs for each day (Figure 4b). The boundary layer at this time generally exhibits a strong stable stratification i.e.,

$\partial\theta/\partial z \gg 0$ . Increased vertical mixing by the additional eddies generated in scenario 2 bring high- $\theta$  air down and low- $\theta$  air up, leading to a warming near the surface and a cooling above the hub height. Obviously this effect is

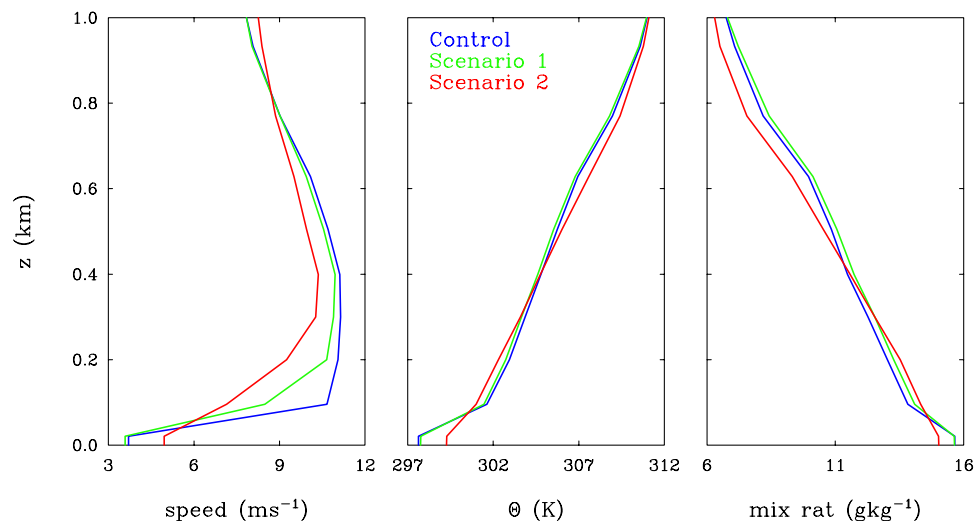


**Figure 4.** Mean vertical profile of horizontal wind speed at 0900 UT (0300 LT),  $\theta$  and total water mixing ratio at 1200 UT (0600 LT) over the wind farm.

**Table 1.** Mean Surface Meteorology

	Control	Scenario 1	Scenario 2
Wind speed, $\text{ms}^{-1}$	3.8	3.7	4.4
Temperature, C	25.8	25.9	26.5
Total water mixing ratio, $\text{g kg}^{-1}$	17.3	17.3	16.6
Sensible heat flux, $\text{Wm}^{-2}$	10.2	11.0	-1.8
Evapotranspiration rate, $\text{mm d}^{-1}$	4.4	4.3	4.7

negligible during daytime when the atmosphere is usually well mixed ( $\partial\theta/\partial z \sim 0$ ). Occasionally, during the daytime, when the atmosphere is very unstable (i.e.,  $\partial\theta/\partial z \ll 0$ ), the turbulent eddies mix cold air down and warm air up, producing a cooler surface.

[24] Similar to that for  $\theta$ , the control and scenario 1 patterns for the near-surface total water mixing ratio ( $R_t$ ) are almost the same (Figure 3d). Scenario 2 produces a drying near the surface and the effect is most prominent in the early morning hours (1200 UT (0600 LT)). Stronger mixing in scenario 2 brings dry air down and moist air up, leading to a drying near the surface and moistening aloft (Figure 4c).

### 3.3. Impact of Wind Farms on Surface Fluxes

[25] While the control and scenario 1 produce almost identical surface flux patterns, scenario 2 is different. The most prominent feature is the significant reduction (tens of  $\text{Wm}^{-2}$ ) in the sensible heat flux (Figure 3e) in the early morning hours. At that time the soil is colder than the atmosphere (negative land-atmosphere thermal gradient) and hence the surface sensible heat flux is negative. The increase in near-surface  $\theta$  due to rotor-generated turbulence makes this gradient more negative, resulting in more sensible heat being transferred from the atmosphere to the ground. Similarly, the drying of the near-surface air by turbulent eddies in scenario 2 cause the positive land-atmosphere moisture gradient to go up further, thereby increasing evapotranspiration (Figure 3f). However, the departures are small, never more than  $0.2 \text{ mmhr}^{-1}$ .

### 3.4. Mean Effects of Wind Farms on Surface Meteorology

[26] The mean impact of wind farms (Table 1), averaged over the entire simulation period, reinforces the observations made in the previous subsections. The surface conditions within the wind farm in scenario 1 are almost identical to that in the control. However, in scenario 2 the surface air experiences moderate warming and drying, as well as an increase in wind speed.

[27] While the differences in evapotranspiration rate is negligible, the impact on the surface sensible heat flux in scenario 2 is strong enough to force a reversal of direction. The soil is cool and wet due to the convective storms that occurred during the first few days of the simulation period and hence, the mean land-atmosphere thermal gradient is negative but small. The increase in surface air temperature reverses this gradient leading to a mean negative sensible heat flux.

### 3.5. Sensitivity of Model Design to Vertical Resolution

[28] A basic requirement of our subgrid parameterization approach is that each hypothetical cylinder be completely contained within a grid cell. We ensure this by making the

thickness of the second atmospheric layer equal to the diameter of the rotors (100 m). This vertical resolution is coarser than that typically used in mesoscale simulations but it does not trigger any numerical instability in our experiments. To test the sensitivity of our model setup to this resolution, we repeat the simulations for 1 day, starting at 1800 UT (1200 LT) 10 July, by doubling the vertical resolutions below 250 m. The hub-height level wind speed was the strongest that night. The low- and high-resolution simulations do not show any difference, implying that the chosen vertical grid is adequate for these experiments.

## 4. Summary and Discussions

[29] This study used a new parameterization to numerically simulate the impacts of a hypothetical wind farm in the Great Plains region on the local meteorology. Results show that wind farms significantly slow down the wind at the turbine hub-height level. Additionally, turbulence generated in the wake of the rotors can enhance vertical mixing that significantly affects the vertical distribution of temperature and humidity as well as surface sensible and latent heat fluxes. The impact is strongest in the early hours of the day primarily due to the strong hub-height level winds associated with the nocturnal low-level jet. Also, the nocturnal boundary layer is stable with large vertical gradients of momentum, humidity and temperature. Under this situation the effect of enhanced vertical mixing is likely to be larger than that in a well-mixed diurnal boundary layer.

[30] A wide range of typical summertime synoptic atmospheric boundary conditions are used in this study and hence, our conclusions regarding the interactions between wind farms and atmospheric flow are generally robust. However, the surface flux signals are probably valid only for relatively wet and cool soil conditions. More work with other types of land surface boundary conditions is required to test the robustness of the surface flux signals.

[31] This study takes into account only localized processes with timescales of the order of days. Processes with longer timescales are important for land-atmosphere interactions. Since high-resolution mesoscale models are computationally expensive, a coarse resolution general circulation model (GCM) can be used to investigate this issue. This will also let us explore the seasonality of the impacts of wind farms on local meteorology.

[32] Observations show that turbine  $C_p$  and rotor-generated turbulence are weak functions of the background wind speed. For simplicity, we assume them to be constants. The sensitivity of our model to these assumptions needs to be tested. Parallel to these modeling exercises, it is imperative that field observations be collected at different wind farms to improve the calibration of our rotor parameterization. Another issue of importance is the relevance of the size of the wind farm. It needs to be seen if the environmental impacts are constant or scale up or down, as the wind farms get larger or smaller.

[33] This is a preliminary study meant to highlight this issue as an interesting problem that requires detailed investigation. The results however can have significant implications for wind power engineering. The findings suggest that reducing rotor-generated turbulence will not only reduce the meteorological impacts of wind farms but also increase the

efficiency. This work also demonstrates that mesoscale modeling can be a source of valuable information with many potential applications including environmental impact assessment, site selection and array design for wind farms.

[34] **Acknowledgments.** We wish to thank N. D. Kelly, National Wind Technology Center, NREL, Golden, CO, and R. H. Williams and D. Denkenberger, Princeton Environmental Institute, Princeton University, Princeton, NJ, for very helpful comments and suggestions. N. D. Kelley also provided the TKE data from San Gorgonio.

## References

- American Wind Energy Association (2002), *Most Frequently Asked Questions About Wind Energy*, Washington, D. C.
- Archer, C. L., and M. Z. Jacobson (2003), Spatial and temporal distribution of U.S. winds and wind power at 80 m derived from measurements, *J. Geophys. Res.*, 108(D9), 4289, doi:10.1029/2002JD002076.
- Best, R. W. B. (1979), Limits to wind power, *Energy Conversion*, 19, 71–72.
- Bonner, W. D. (1968), Climatology of the low level jet, *Mon. Weather Rev.*, 96, 833–850.
- Cavallo, A. J., S. M. Hock, and D. R. Smith (1993), Wind energy: Technology and economics, in *Renewable Energy*, edited by T. B. Johansson et al., pp. 121–156, Island Press, Washington, D. C.
- Cotton, W., et al. (2003), RAMS 2001: Current status and future directions, *Meteorol. Atmos. Phys.*, 82, 5–29.
- Frandsen, S. (1992), On the wind speed reduction in the center of large clusters of wind turbines, *J. Wind Eng. Indust. Aerodyn.*, 39, 251–265.
- Grubb, M. J., and N. I. Meyer (1993), Wind energy: Resources, systems and regional strategies, in *Renewable Energy*, edited by T. B. Johansson et al., pp. 157–212, Island Press, Washington, D. C.
- Intergovernmental Panel on Climate Change (IPCC) (2001), *Climate Change 2001*, edited by J. T. Houghton et al., 881 pp., Cambridge Univ. Press, New York.
- Ivanova, L. A., and E. D. Nadyozhina (2000), Numerical simulation of wind farm influence on wind flow, *Wind Eng.*, 24, 257–269.
- Kalnay, E., et al. (1996), The NCEP/NCAR 40-year reanalysis project, *Bull. Am. Meteorol. Soc.*, 77, 437–471.
- Leclerc, C., C. Masson, I. Ammara, and I. Paraschivoiu (1999), Turbulence modeling of the flow around horizontal axis wind turbines, *Wind Eng.*, 23, 279–294.
- Magnusson, M. (1999), Near-wake behavior of wind turbines, *J. Wind Eng. Indust. Aerodyn.*, 80, 147–167.
- Malyshev, S. L., S. W. Pacala, D. W. Keith, D. C. Denkenberger, S. Baidya Roy, and E. Shevliakova (2003), Climate response to large-scale wind farms, *Eos Trans. AGU*, 84(46), Fall Meet. Suppl., Abstract A31E-0104.
- Mellor, G. L., and T. Yamada (1982), Development of a turbulence closure model for geophysical fluid problems, *Rev. Geophys.*, 20, 851–875.
- National Wind Coordinating Committee (1997), Wind energy environmental issues, *NWCC Issue Brief 2*, Washington, D. C.
- Office of Energy Efficiency and Renewable Energy (EERE) (2002), *Wind Power Today: Wind Energy Research Highlights*, Dept. of Energy, Washington, D. C.
- Peixoto, J. P., and A. H. Oort (1992), *Physics of Climate*, 520 pp., Am. Inst. of Phys., New York.
- Petersen, E. L., N. G. Mortensen, L. Landberg, J. Hojstrup, and H. P. Frank (1998), Wind power meteorology. Part I: Climate and turbulence, *Wind Energy*, 1, 25–45.
- Pielke, R. A., W. R. Cotton, R. L. Walko, C. J. Tremback, M. E. Nicholls, M. D. Moran, D. A. Wesley, T. J. Lee, and J. H. Copeland (1992), A comprehensive meteorological modeling system—RAMS, *Meteorol. Atmos. Phys.*, 49, 69–91.
- Stull, R. B. (1988), *An Introduction to Boundary Layer Meteorology*, 666 pp., Kluwer Acad., Norwell, Mass.
- Taylor, G. L. (1983), Wake and performance measurements on the Lawson-Tancred 17 m horizontal-axis windmill, *IEE Proc.*, 130, 604–612.
- Walko, R. L., et al. (2000), Coupled atmosphere-biophysics-hydrology model for environmental modeling, *J. Appl. Meteorol.*, 39, 931–944.
- Weaver, C. P., and R. Avissar (2001), Atmospheric disturbances caused by human modification of the landscape, *Bull. Am. Meteorol. Soc.*, 82, 269–281.

S. Baidya Roy and S. W. Pacala, Department of Ecology and Evolutionary Biology, Princeton University, Princeton, NJ 08540, USA. (sroy@princeton.edu; pacala@princeton.edu)

R. L. Walko, Department of Civil Engineering, Duke University, Durham, NC 27708-0287, USA. (robert.walko@duke.edu)